Journal of Hazardous Materials 185 (2011) 914–921

Contents lists available at ScienceDirect

Journal of Hazardous Materials

journal homepage: www.elsevier.com/locate/jhazmat

Study on adsorption and desorption properties of the starch grafted p-tert-butyl-calix[*n*]arene for butyl Rhodamine B solution

Ming Chen[a,b], Ting Shang[a,b], Wei Fang[a,b], Guowang Diao[a,b,*]

[a] College of Chemistry and Chemical Engineering, Yangzhou University, Yangzhou 225002, PR China
[b] Key Laboratory of Environmental Materials & Environmental Engineering of Jiangsu Province, Yangzhou, Jiangsu, 225002, PR China

ARTICLE INFO

Article history:
Received 22 June 2010
Received in revised form 21 August 2010
Accepted 28 September 2010
Available online 7 October 2010

Keywords:
Adsorption
Desorption
p-Tert-butyl-calix[4,6,8]arene
Starch
Butyl Rhodamine B
Adsorption isotherm

ABSTRACT

The adsorbents of starch grafted p-tert-butyl-calix[4,6,8]arene-SGCn (SGC4, SGC6, SGC8) are prepared. The products are characterized by FTIR, elemental analysis, thermal gravimetric analysis and scanning electron microscope. Static adsorption behavior is studied by using SGC8 as adsorbent, butyl Rhodamine B (BRB) solution as simulation dye wastewater. The adsorption of BRB onto SGC8 fits the second order kinetic model and the apparent adsorption rate constant is 0.002 g mg^{-1} min^{-1} at 25 °C. The equilibrium adsorption data are interpreted using Langmuir and Freundlich models. The adsorption of BRB onto SGC8 is better represented by the Langmuir equation. The thermodynamic parameters for the adsorption reaction are calculated through van't Hoff analysis. The adsorbent may be easily regenerated by using ethanol solution as desorption agent to extract dye from SGC8. The rate of desorption of BRB is dependent on the concentration of ethanol and the temperature. SGC8 exhibits excellent adsorption and desorption properties toward dye molecule. The new-style adsorbent of SGC8 is regarded as a potential adsorbent to deal with dye or organic wastewater.

1. Introduction

Dyes and pigments are widely used, mostly in leathers, textiles, paper mill, additives, foodstuff and cosmetics industry to color products. Today, they are considered as a kind of extremely important pollutant in environment due to their complex composition, high toxicity, poor degradability and great solubility in water [1,2]. Hence, the removal of dye from colored reactive dye wastewater is an important environmental issue.

The most commonly methods for the color removal include physicochemical, chemical, and biological methods, such as coagulation [3,4], precipitation [5], adsorption, filtration [6], membrane separation [7,8], chemical oxidation [9,10], ion-exchange [11,12], and aerobic and anaerobic microbial degradation [13,14]. Among these methods, liquid-phase adsorption processes are efficient for removal of dye pollutants from the industrial wastewater. More researches have been done on the adsorption behaviors of dyes in aqueous solution by adsorbents such as resins [15], chitosan [16], activated carbon [17], titanium phosphate [18], zeolites [19], iron oxides [20] and clay [21], have been reported in the literature.

Recently, much more attention has been paid to chemical separation techniques and the design and synthesis of new extraction reagents for ions and molecules. The attention results from environmental concerns and efforts to save energy and enhance recycling at the industrial level. In this respect, supramolecular chemistry has provided important avenues to prepare new type adsorbents and extraction reagents. This was achieved with the development of macrocyclic receptors, such as crown ethers [22,23], cyclodextrins [24–33] and calix[*n*]arenas [34–38]. Calix[*n*]arenes are cyclic oligomers synthesized by condensation of a p-alkylated phenol and formaldehyde. Calixarenes have a particular configuration because of its cavity. It has the flexibility to adjust the cavity dimension and the ability to form inclusion compounds with a great variety of guests, from charged molecules such as anions, metallic cations to apolar compounds. This versatility makes the calixarene family the third major class of macrocyclic binding agents after crown-ethers and cyclodextrins [39–41]. Nowadays many researchers are interested in crosslinking calixarenes with suitable crosslinkers to form an insoluble resin which has specific adsorption based on inclusion complex formation [34–38].

In this article, starch has received a considerable attention as basic matrixes for designing new adsorbent. p-Tert-butyl-calix[4,6,8]arene are grafted onto starch through epichlorohydrin to prepare adsorbents-SGCn (SGC4, SGC6, SGC8). To research the adsorption capacity and mechanism of adsorbent, butyl Rhodamine B is chosen as adsorbate (the structure is shown in Fig. 1(A)).

* Corresponding author at: College of Chemistry and Chemical Engineering, Yangzhou University, Yangzhou 225002, PR China. Tel.: +86 514 87975436; fax: +86 514 87975244.
E-mail address: gwdiao@yzu.edu.cn (G. Diao).

0304-3894/$ – see front matter © 2010 Elsevier B.V. All rights reserved.
doi:10.1016/j.jhazmat.2010.09.107

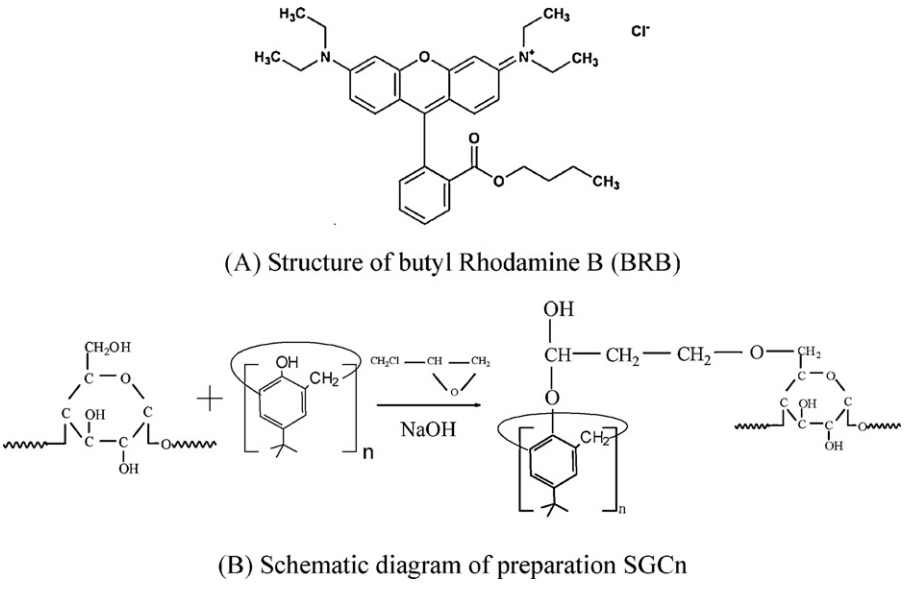

(A) Structure of butyl Rhodamine B (BRB)

(B) Schematic diagram of preparation SGCn

Fig. 1. (A) Structure of butyl Rhodamine B (BRB). (B) Preparation of adsorbents of starch grafted p-tert-butyl-calix[4,6,8]arene (SGCn).

Rhodamine B (RhB), Basic Violet 10, is a highly water soluble, non-volatile, basic dye of the xanthene class. It is widely used in industry as a colorant in textile, leather, jute and food industries, and is also a well-known water tracer fluorescent [42]. However, it causes phototoxic and photoallergic reactions, which have toxic, carcinogenic or mutagenic influences on living organisms [43]. Therefore, the dye-containing wastewater should be treated before discharge. The adsorption behavior of BRB onto SGC8 is studied. The cavity size effect of calixarene for the adsorption capacity is first reported. The kinetics and thermodynamic parameters for the adsorption reaction are calculated through static adsorption study. The adsorbent is regenerated by using ethanol solution as desorption agent to extract dye from SGC8. The desorption efficiency and regeneration capability are investigated and the results show that SGC8 is regarded as a potential adsorbent to deal with dye sewage.

2. Experimental

2.1. Reagent

p-Tert-butyl-calix[*n*]arene (*n* = 4, 6, 8) are synthesized according to references [44,45]. Butyl Rhodamine B (BRB) is purchased from Shanghai Chemical Reagents Company and used without purification. Starch (AR), epichlorohydrin (AR) is obtained from Sinopharm Chemical Reagent Company and used without any purification. Highly pure water is obtained from a Millipore Milli-Q UV system.

2.2. Instrument

FTIR spectra for the different samples are recorded on a Bruker TENSOR 27 FTIR spectrometer operated at a resolution of 4 cm^{-1}. Elemental analysis for adsorbents is measured by using a SERIES II2400 (PerkinElmer) elemental analyzer. The thermal analysis of samples is characterized by thermal gravimetric analysis (TGA) on a STA409PC TGA instrument (Netzsch, Germany) with a heating rate of 10 °C min^{-1}. The morphology and size of adsorbent are investigated by a Philips XL-30ESEM scanning electron microscope (SEM) instrument operated at an accelerating voltage of 20 kV. Fluorescence spectra are operated by F4500 (Shimazu, Japan) using a conventional 1 cm × 1 cm quartz cell in a thermostated compartment. The excitation wavelength is 490 nm. Adsorption and desorption experiments are completed on a laboratory shaker HZ-9211K (Jiangsu, China).

2.3. Preparation of adsorbents

The preparation scheme of SGC8 is shown in Fig. 1(B). The procedure is described briefly as follows: a mixture of starch (1.00 g), p-tert-butyl-calix[8]arene (4.00 g), and sodium hydroxide aqueous solution (6 mL, 20%) is stirred at 50 °C. Then, epichlorohydrin (30 mL) is dropped into above mixture and the mixed system is stirred at 50 °C for 24 h. The product is filtered and washed in sequence with ethanol and acetone three times. The precipitate is dried in a vacuum oven at 50 °C for 24 h. At the end, yellow powder is obtained and characterized by FTIR, elemental analysis and SEM. SGC4 and SGC6 are synthesized by the same method.

2.4. Adsorption and desorption experiments

The influence of the initial solution pH on the adsorption capacity of BRB onto SGC8 is studied. Adsorption experiments are done by agitating 50 mL of dye solution at different pH (20 mg L^{-1}) with fresh SGC8 200 mg in glass bottles using a laboratory shaker at 180 rpm and the room temperature (25 ± 1 °C). The equilibrium adsorption amount of BRB onto SGC8 at different pH is estimated by monitoring the residual BRB in the solution at the maximum emission wavelength (599 nm) by using a Fluorescence spectrophotometer. The equilibrium adsorption amount of SGC8, q_e (mg g^{-1}), is calculated using the following relationship [46,47]:

$$q_e = \frac{(c_0 - c_e)V}{W} \quad (1)$$

where c_0 is the initial concentration of BRB (mg L^{-1}), c_e is the equilibrium concentration of dye (mg L^{-1}), V is the volume of the solution (L), and W is the mass of the SGC8 (g).

To research adsorption kinetic behavior of BRB onto SGC8, batch adsorption experiments are done by agitating 50 mL of dye solution (20 mg L^{-1}, pH = 8) with fresh SGC8 200 mg in glass bottles using a laboratory shaker at 180 rpm and the room temperature (25 ± 1 °C). At different adsorption time, the dye solution is separated from the adsorbent by centrifugation at 8000 rpm for 5 min. The adsorption amount of BRB onto SGC8 at different adsorption time is estimated by monitoring the residual BRB in the solution at the maximum

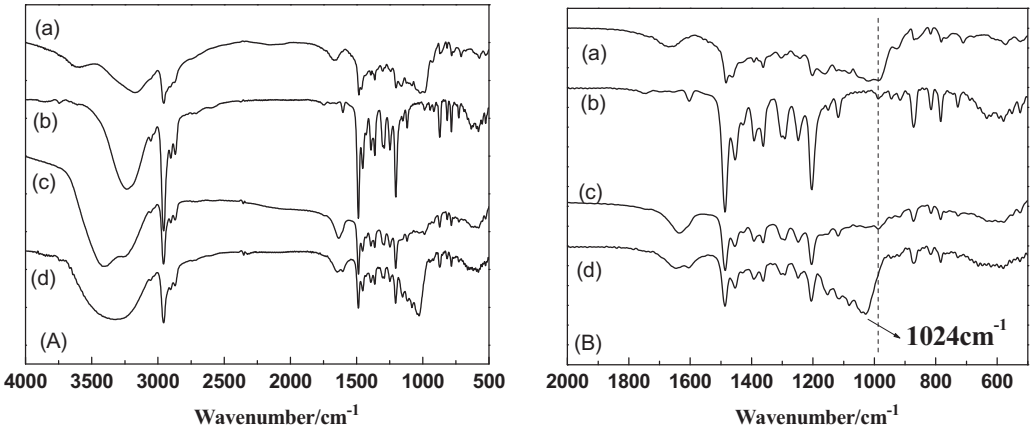

Fig. 2. FT-IR spectra of (a) starch, (b) p-tert-butyl-calix[8]arene, (c) their mixture, (d) SGC8: (A) in the range of 4000–500 cm^{-1}; (B) in the range of 2000–500 cm^{-1}.

emission wavelength (599 nm) by using a fluorescence spectrophotometer.

Adsorption isotherms are obtained by using a batch equilibration technique at different temperature.

The adsorption efficiency (%), is calculated using the following relationship:

$$\eta_A = \frac{q_e}{q_m} \times 100\% \quad (2)$$

where q_e ($mg\,g^{-1}$) is the equilibrium adsorption capacity of SGC8 and q_m ($mg\,g^{-1}$) is the saturation adsorption capacity.

In desorption experiment, 2 g fresh SGC8 is put in 1 L 80 $mg\,L^{-1}$ BRB aqueous solution. The solution above is shaken by laboratory shaker (180 rpm) 5 h at 25 °C to make an equilibrium absorption of BRB onto SGC8, which is filtrated and dried at room temperature for further use. The adsorption capacity is about 12 $mg\,g^{-1}$. Then, 0.1 g above SGC8 is added into conical flasks. The different concentration of ethanol solution is used as desorption agent and the volume is 20 mL. At desorption equilibrium, the concentration of BRB in desorption agent phase is measured by fluorescence spectra as previously described.

The desorption efficiency (%), is calculated using the following relationship:

$$\eta_D = \frac{c_{e,D}V}{q_m W} \times 100\% \quad (3)$$

where $c_{e,D}$ ($mg\,L^{-1}$) is the desorption equilibrium concentration of dye, V (L) is the volume of the desorption agent solution, q_m ($mg\,g^{-1}$) is the saturation adsorption capacity and W (g) is the mass of the SGC8.

In a typical regeneration experiment, the 80% ethanol solution is used as desorption agent and the volume is 20 mL. 0.1 g SGC8 covered with BRB is dipped in turn in fresh desorption agent for 10×. The adsorption and desorption efficiency is calculated by using Eqs. (2) and (3).

3. Results and discussion

3.1. Characterization of adsorbents

The FTIR spectra of starch, p-tert-butyl calix[8]arene, their mixture and SCG8 are taken by FTIR spectrometer with a KBr film and shown in Fig. 2. Fig. 2(a) shows the FTIR spectrum of starch. The band observed at 3460 cm^{-1} is assigned to –OH stretching vibration. For p-tert-butyl calix[8]arene, the characteristic vibration peaks of –OH at 3244 cm^{-1}, $-C(CH_3)_3$ stretching vibration at 2957 cm^{-1}, phenyl plane bending vibrations at 1608, 1485 cm^{-1} are clearly observed in Fig. 2(b). All above absorption peaks can be found in Fig. 2(c). However, in Fig. 2(d), the band observed at 2957 cm^{-1} is assigned to the p-tert-butyl stretching vibration, which indicates powerful that p-tert-butyl-calix[8]arene is immobilized on starch. Furthermore, compared with the mechanical mixture (shown in Fig. 2B(c)), the band observed at 1024 cm^{-1} is assigned to stretching vibration of C–O–C (shown in Fig. 2B(d)), which provides a substantial evidence of grafting of p-tert-butyl calix[8]arene onto the starch. The FT-IR spectra of SCG4 and SCG6 are shown in Figs. S1 and S2.

The result of elemental analysis further confirmed the immobilized p-tert-butyl-calix[8]arene on starch. Elemental analysis for p-tert-butyl-calix[8]arene (molecular formula:$(C_{11}H_{14}O)_8$): C, 81.37%, H, 9.11%. The ratio of C:H is very close to theoretic value of p-tert-butyl-calix[8]arene (81.48:8.64). Elemental analysis for starch (molecular formula $(C_6H_{10}O_5)_n$): C, 41.65%, H, 6.46%. Elemental analysis for SGC8: C, 44.59%, H, 6.89%. The contents of carbon and hydrogen increase slightly, which indicates that the p-tert-butyl-calix[8]arene is immobilized on starch. Elemental analysis for SGC4 and SGC6 is listed in Table S1. The contents of carbon and hydrogen increase with the number of p-tert-butyl-phenol.

As shown in Fig. 3, thermal gravimetric analysis (TGA) is used to analyze the thermostability of SGC. For starch, two main steps shown in Fig. 3(a) are observed. The first step ranging from 45 to 139 °C is due to the loss of moisture. The second ranging from 278 to 335 °C is assigned to the breakage of starch backbone. Two main steps on thermal degradation curves for p-tert-butyl-calix[8]arene are shown in Fig. 3(b). The first step ranging from 366 to 410 °C is assigned to the loss of the functional group of p-tert-butyl in

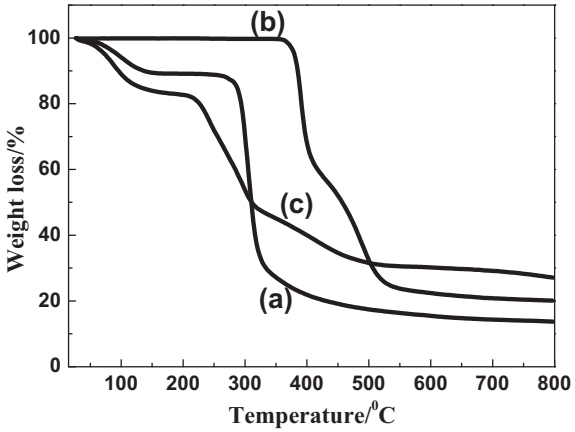

Fig. 3. TGA curves (a) starch, (b) p-tert-butyl calix[8]arene, (c) SGC8.

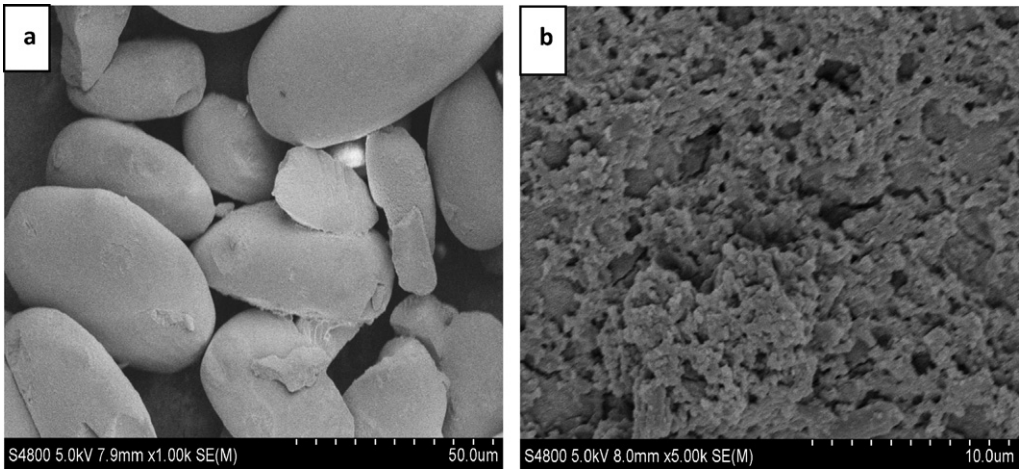

Fig. 4. SEM micrograph of (a) starch, (b) SGC8.

calixarene. The weight loss is about 38% which is similar to the theoretic value. The second step ranging from 410 to 524 °C is attributed to the breakage of the ring of the calix[8]arene. The TGA curve of SGC8 is shown in Fig. 3(c). The thermal degradation for SGC is more complicated and three main steps are observed clearly. The first and second steps ranging from 40 to 125 °C and 215–321 °C are similar to that observed for thermal degradation of starch shown as in Fig. 3(a). The degradation ranging from 321 to 530 °C may be assigned to the degradation of calix[8]arene grating onto the polymer. Thermal degradation curves for SGC4 and SGC6 are presented in Fig. S3. Compared with SGC8, the shape of the thermal degradation curves is quite similar. But the weight loss increases in the order of the size of the calixarene ring, i.e., SGC4 < SGC6 < SGC8.

Fig. 4 shows the SEM micrograph of starch (a) and SGC8 (b). It is clear that the morphology of starch changes a lot after p-tert-butyl-calix[8]arene immobilized on the surface of carrier, which provides an assistive technology support of grafting of p-tert-butyl calix[8]arene onto starch. The morphology of SGC4 (a) and SGC6 is similar to that of SGC8 and the SEM micrograph of SGC4 (a) and SGC6 (b) are shown in Fig. S4.

3.2. Adsorption behavior of BRB onto SGCn

3.2.1. Effect of pH

The value of pH is known as one of the most important factors affecting adsorption capacity of adsorbents. Fig. 5 shows the influence of the initial solution pH on the adsorption capacity of BRB onto SGC8. From Fig. 5, the adsorption capacity of BRB onto SGC8 increases with the pH while the value of pH changes from 2 to 9. There is slight increase in the adsorption capacity at low acidity. On the contrary, the significant change in the adsorption capacity at the high value of pH is shown in Fig. 5. The largest adsorption capacity is 9.81 mg g^{-1} at pH = 9.0. Several investigations report that adsorption quantity of basic dye usually increases as the pH is increased [48,49]. Basically, at lower value of pH, positively charged surface sites on the adsorbent do not favor the adsorption of dye cations due to the electrostatic repulsion. At high pH, OH^- on the surface of adsorbent will favor the adsorption of cationic dye molecules. However, in the application of dye wastewater treatment, the value of pH of dye solution is always regulated to neutral. Therefore, from the results of experiment and practical application, pH = 8.0, weak alkalinity, is chosen as the appropriate value of the initial solution of BRB.

3.2.2. Kinetic behavior of adsorption

From batch adsorption experiments, the adsorption capacity of BRB onto starch, SGC4, SGC6 and SGC8 at different adsorption time are shown in Fig. 6. It clearly shows that the adsorption capacity of starch, SGC4 and SGC6 is increased slowly with the time during the first 60 min and adsorption equilibrium reach after 100 min. However, when SCG8 is used as adsorbent, the adsorption capacity

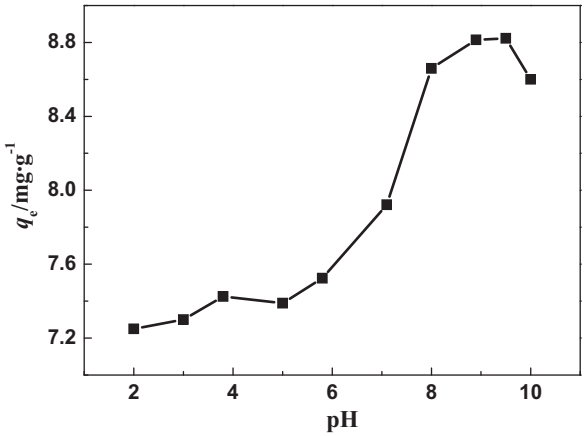

Fig. 5. At 25 °C, adsorption capacity of BRB onto SGC8 at different pH.

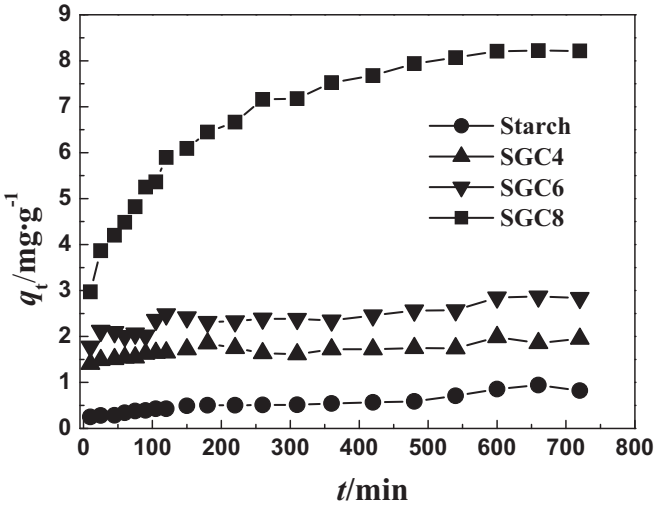

Fig. 6. The relationship between q_t and t of different adsorbents.

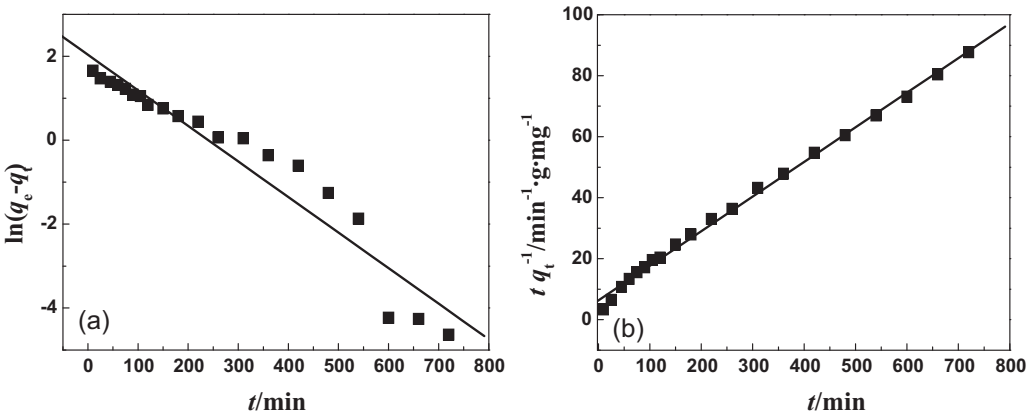

Fig. 7. (a) The relationship between $\ln(q_e - q_t)$ versus t. (b) The relationship between (t/q_t) versus t.

is increased rapidly with the time and an adsorption equilibrium reaches after 600 min. It is evident that the equilibrium adsorption capacity of SGC8 is further larger than that of starch, SGC4 and SGC6. So, SGC8 is chosen the main object of study.

Many kinetic models are developed in order to find intrinsic kinetic adsorption constants. Traditionally, the kinetics of metal ions adsorption is described following the expressions originally given by Lagergren which are special cases for the general Lagergren rate equation [50]. A simple kinetic analysis of adsorption is the pseudo-first-order equation in the form:

$$\ln(q_e - q_t) = -k_1 t + \ln q_e \tag{4}$$

where k_1 (min^{-1}) is adsorption rate constant, q_e and q_t ($\mathrm{mg\,g}^{-1}$) adsorption capacity of dye adsorbed at equilibrium and at any time, respectively.

A pseudo-second-order equation based on adsorption equilibrium capacity may be expressed as follows [51,52]:

$$\frac{t}{q_t} = \frac{1}{k_2 q_e^2} + \frac{t}{q_e} \tag{5}$$

where k_2 ($\mathrm{g\,mg}^{-1}\,\mathrm{min}^{-1}$) is adsorption rate constant of a pseudo-second-order equation.

The fitting validity of these models is traditionally checked by each linear plot of $\ln(q_e - q_t)$ versus t, and (t/q_t) versus t, respectively. Fig. 7(a) and (b) show the fitting plots of two kinetic models. From correlation coefficients, the value of R^2 in the second-order kinetic model (0.997) is higher than the first-order kinetic model value (0.927), which indicates that the adsorption of BRB onto SGC8 fits a pseudo-second-order reaction. From the slope and intercept of the straight line (Fig. 7(b)), the pseudo-second-order rate constant k_2 is evaluated as $0.002\,\mathrm{g\,mg}^{-1}\,\mathrm{min}^{-1}$.

3.2.3. Adsorption isotherms

The adsorption isotherms of BRB onto starch, SGC4, SGC6 and SGC8 at 25 °C are shown in Fig. 8(a). Comparing adsorption capacity of four adsorbents at 25 °C, the saturation adsorption capacity increases in the order of starch, SGC4, SGC6 and SGC8. In three starch-calix[8]arene polymer, the saturation adsorption capacity of SGC8 is larger than that of SGC4 or SGC6, which is attributed to the larger formation constant between calix[8]arene and BRB (The formation constants between calix[4,6,8]arene and BRB are calculated by fluorescence spectroscopy). Therefore, the larger formation constant between calixarene and guest molecule is, the larger adsorption capacity of the adsorbent is.

The adsorption isotherms of BRB onto SGC8 at different temperature are shown in Fig. 8(b). The Langmuir sorption isotherm is the most widely used for the adsorption of a pollutant from a liquid solution assuming that the adsorption takes place at specific homogeneous sites within the adsorbent [53,54]. Assuming the adsorption coincided with Langmuir's model, the Langmuir adsorption isotherm is expressed by the following equation [53,54]:

$$\theta = \frac{q_e}{q_m} = \frac{K_L c_e}{1 + K_L c_e} \tag{6}$$

where θ is coverage, c_e ($\mathrm{mg\,L}^{-1}$) and q_e ($\mathrm{mg\,g}^{-1}$) are the liquid phase concentration and solid phase concentration of sorbent at equilibrium, respectively; q_m ($\mathrm{mg\,g}^{-1}$) is the saturation adsorption capacity and K_L ($\mathrm{L\,mg}^{-1}$) is the Langmuir isotherm constant.

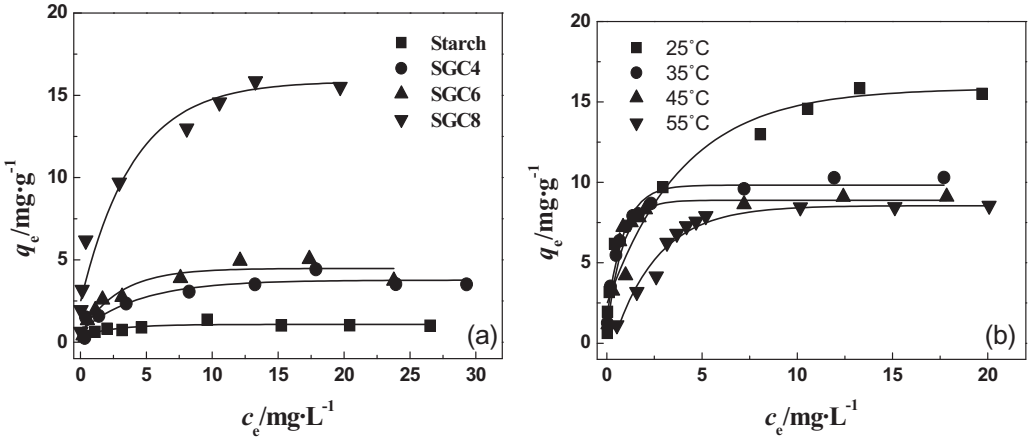

Fig. 8. (a) At 25 °C, adsorption isotherm for BRB onto different adsorbents. (b) Adsorption isotherm for BRB onto SCG8 at different temperature.

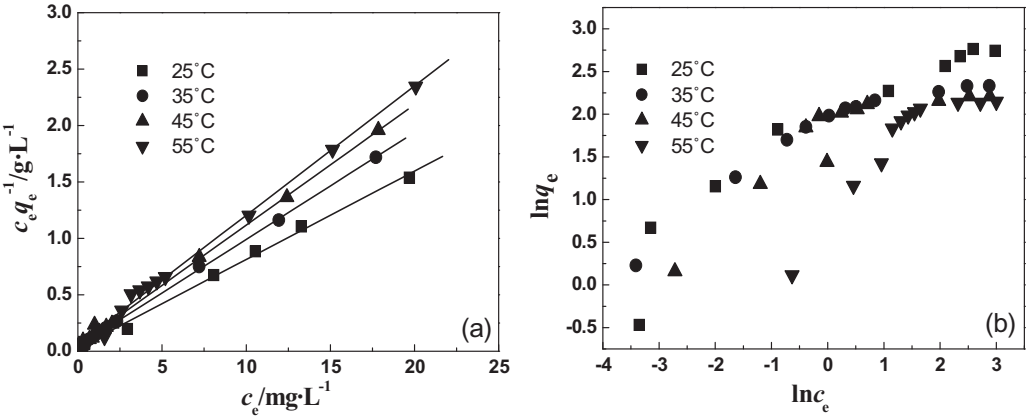

Fig. 9. (a) The relationship between c_e/q_e and c_e at different temperature. (b) The relationship between lnq_e and lnc_e at different temperature.

The linear equation of Langmuir is represented as follows:

$$\frac{c_e}{q_e} = \frac{c_e}{q_m} + \frac{1}{K_L q_m} \quad (7)$$

Fig. 9(a) shows the relationships between c_e/q_e and c_e at different temperature. A well behaved linear relationship implies that adsorption of BRB onto SGC8 obeys Langmuir's model. According to the slope and the intercept of the straight lines, q_m and K_L both can be evaluated. Table 1 lists the values of q_m, K_L and R^2 (R, the correlation coefficient) at different temperature for Langmuir isotherm. From the value of R^2, the adsorption system under the concentration range studied fits Langmuir isotherm well. From Table 1, both q_m and K_L are dependent on the temperature. With the temperature increasing, the values of q_m and K_L decrease gradually, which indicates that the higher temperature, the more disadvantageous for the adsorption of BRB onto SGC8.

It is well known that the Freundlich isotherm is the earliest known relationship describing the adsorption equation [55]. The application of the Freundlich equation suggests that sorptional energy exponentially decreases on completion of the adsorption centers of a sorbent. This isotherm is an empirical equation employed to describe heterogeneous systems and is expressed by the following equation:

$$q_e = K_F c_e^{1/n} \quad (8)$$

where q_e is the equilibrium dye concentration onto adsorbent (mg g^{-1}), c_e is the equilibrium dye concentration in solution (mg L^{-1}), K_F is Freundlich constant, and $1/n$ is the heterogeneity factor. The capacity constant K_F and the affinity constant n are empirical constants dependent on several environmental factors. A linear form of the Freundlich expression can be obtained by taking logarithms of Eq. (9):

$$\ln q_e = \ln K_F + \frac{1}{n} \ln c_e \quad (9)$$

The plot of ln q_e versus ln c_e is shown in Fig. 9(b). Table 1 lists the values of K_F, n and R^2 at different temperature for Freundlich isotherm.

Table 1
At different temperature adsorption constants and the correlation coefficients for Langmuir and Freundlich isotherm.

T/K	Langmuir isotherm			Freundlich isotherm		
	K_L/L mg^{-1}	q_m/mg g^{-1}	R^2	K_F	n	R^2
298	2.66	12.76	0.997	5.53	2.39	0.888
308	2.25	10.54	0.998	5.81	3.22	0.846
318	2.11	9.37	0.998	5.10	3.13	0.721
328	1.93	8.73	0.994	2.56	1.87	0.785

From the value of R^2, the linear relationship dose not fit well for the adsorption system under the concentration range studied. Apparently, this plot demonstrates that equilibrium adsorption data of BRB is not excellent for the Freundlich isotherm. It is evident that the Langmuir model is better than the Freundlich model in this case. The Langmuir equation is applicable to homogeneous adsorption, where the adsorption of each molecule onto the surface has equal adsorption activation energy. This suggests that some homogeneity in the surface of sorbent will play a key role in dye adsorption and that the homogeneous adsorption model will be better for isotherm simulation. The value of the monolayer saturation capacity indicates that SGC8 exhibits interesting adsorption properties toward dye molecule and SGC8 will be a potential adsorbent for dealing with dye or organic wastewater.

3.2.4. Thermodynamics parameters of adsorption reaction

To elucidate the thermodynamic origins of the adsorption reaction of BRB onto SGC8, the thermodynamic parameter for the adsorption reaction is determined through van't Hoff analysis. The relationship of the Langmuir isotherm constant K_L with temperature T can be described by van't Hoff equation shown as follows:

$$\ln K_L = -\frac{\Delta H^\theta}{RT} + \frac{\Delta S^\theta}{R} \quad (10)$$

where R is the gas constant, ΔH^θ is the enthalpy change and ΔS^θ is the entropy change. The K_L (L g^{-1}) has to be converted to K_L' (L mol^{-1}) by using the molecular weight of BRB before calculating ΔH^θ and ΔS^θ [56]. ΔH^θ (kJ mol^{-1}) and ΔS^θ (J mol^{-1} K^{-1}) are calculated from the slope and intercept of linear plot of ln K_L' versus T^{-1} (the plot is shown in Fig. 10).

The Gibbs free energy change, ΔG^θ, is estimated from the following relationship:

$$\Delta G^\theta = \Delta H^\theta - T\Delta S^\theta \quad (11)$$

The thermodynamic parameter for the adsorption reaction is determined through van't Hoff analysis. The good linear relationship between ln K_L' and $1/T$ is obtained (Fig. 10), and therefore the value of the molar enthalpy, the entropy change and the Gibbs free enthalpy change is calculated −8.41 kJ mol^{-1}, −7.25 J mol^{-1} K^{-1} and −6.25 kJ mol^{-1}, respectively. The adsorption reaction of BRB onto SGC8 is driven by the favorable enthalpic change, accompanying negative entropy change. The negative value of molar enthalpy change indicates that the adsorption reaction is exothermic reaction, so higher temperature is disadvantageous to the adsorption reaction. The negative value of entropy change is due to the decrease of the freedom of dye molecule after the adsorption of BRB onto SGC8.

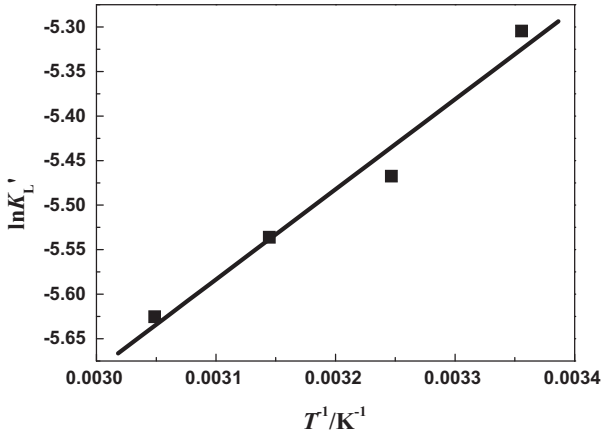

Fig. 10. Relationship between $\ln K_L'$ and T^{-1}.

Table 2
The desorption efficiency (%) with different concentration of ethanol solution as desorption agent.

	Ethanol/%				
	0	20	40	60	80
Desorption efficiency/%	1.97	23.6	54.1	71.4	99.7

3.3. Desorption of BRB from SGC8

3.3.1. Effect of concentration of desorption agent

In desorption experiment, the different concentration of ethanol solution is used as desorption agent. The desorption equilibrium time is about 9 h. The rate of desorption (%), is calculated by Eq. (3) and the result is shown in Table 2. It indicates that the rate of desorption depends on the concentration of ethanol. When the concentration of ethanol is 80%, the desorption efficiency is close to 100%, which reveals that higher concentration of ethanol is good desorption agent.

3.3.2. Temperature dependence of the desorption

Fig. 11 shows the rate of desorption at different temperature with 40% ethanol solution. The amount of BRB desorbed from SGC8 depends on the temperature. It is clear that the desorption efficiency of BRB from SGC8 increases with temperature, which demonstrates that higher temperature is advantageous to the desorption reaction.

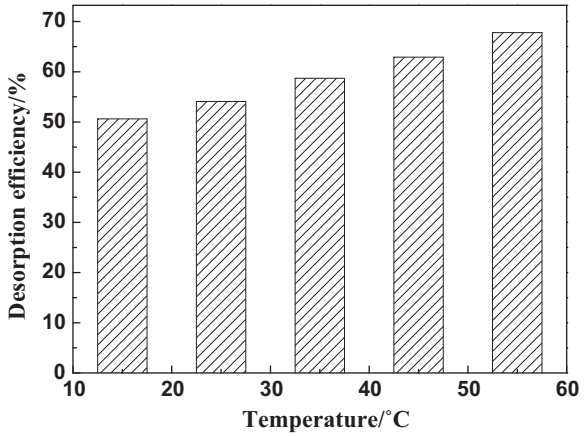

Fig. 11. The plot of the desorption efficiency at different temperature using 40% ethanol solution as desorption agent.

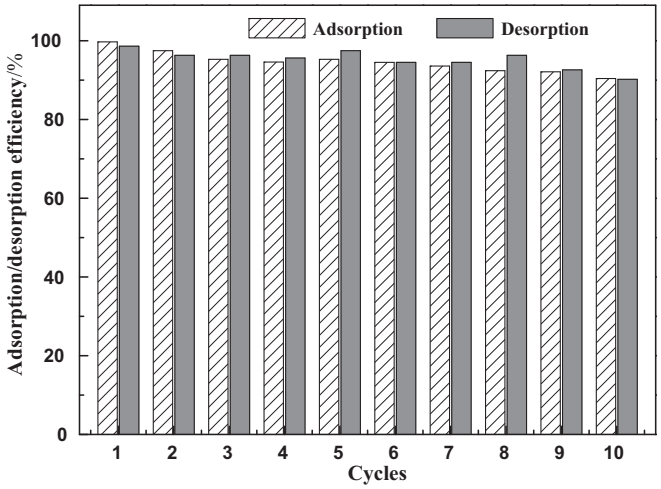

Fig. 12. The adsorption/desorption efficiency of cycles for BRB onto SCG8 at 25 °C.

3.3.3. Regeneration of the adsorbent

To the practical application of the adsorption process using SGC8, it is necessary to study the regeneration of the adsorbent. 80% ethanol solution is used as desorption agent for SGC8 regeneration. The adsorbent is used 10 times repeatedly and the rates of adsorption and desorption are shown in Fig. 12. With the increasing of the repeated times, the rates of adsorption and desorption are decreased slightly. It is found that SGC8 can be used repeatedly without significant decline of its adsorption capabilities during adsorption–desorption cycles. However, using ethanol solution as desorption agent will cause secondary pollution and the cost is too expensive. Therefore, if the desorption agent is improved, SGC8 can be regarded as a potential adsorbent in the application of sewage treatment.

4. Conclusions

The adsorbents of starch grafted p-tert-butyl-calix[4,6,8]arene-SGCn (SGC4, SGC6, SGC8) are synthesized successfully. The adsorption of BRB onto SGC8 fits the second order kinetic model. The order of the saturation adsorption capacity at 25 °C is consistent with the size of the calixarene ring, i.e., SGC4 < SGC6 < SGC8. The adsorption behavior of BRB onto SGC8 obeys Langmuir's model. The thermodynamic parameters indicate that the adsorption reaction of BRB onto SGC8 is driven by the favorable enthalpic change, accompanying negative entropy change. The desorption efficiency of BRB is dependent on the concentration of ethanol and the temperature. The adsorbent may be easily regenerated by using 80% ethanol solution as desorption agent to extract dye from SGC8. The adsorbent of SGC8 can be regarded as a potential adsorbent in the application of dye or organic wastewater treatment.

Acknowledgements

The authors acknowledge the financial support from the National Natural Science Foundation of China (Grant Nos. 20773107, 20973151, 20901065), the Natural Science Key Foundation of Educational Committee of Jiangsu Province of China (Grant No. 07KJA15015), the Specialized Research Fund for the Doctoral Program of Higher Education (SRFDP, 20093250110001), the Foundation of Jiangsu Provincial Key Program of Physical Chemistry in Yangzhou University and the Foundation of the Educational Committee of Jiangsu Provincial Universities Excellence Science and Technology Invention Team in Yangzhou University.

Appendix A. Supplementary data

Supplementary data associated with this article can be found, in the online version, at doi:10.1016/j.jhazmat.2010.09.107.

References

[1] J. García-Montaño, X. Xavier Domènech, J.A. García-Hortal, F. Torrades, J. Peral, The testing of several biological and chemical coupled treatments for Cibacron Red FN-R azo dye removal, J. Hazard. Mater. 154 (2008) 484–490.
[2] Y. Li, A.H. Lua, S. Jin, C.Q. Wang, Photo-reductive decolorization of an azo dye by natural sphalerite: case study of a new type of visible light-sensitized photocatalyst, J. Hazard. Mater. 170 (2009) 479–486.
[3] C. Allegre, M. Maisseu, F. Charbit, P. Moulin, Coagulation–flocculation–decantation of dye house effluents: concentrated effluents, J. Hazard. Mater. B116 (2004) 57–64.
[4] S.S. Moghaddam, M.R.A. Moghaddam, M. Arami, Coagulation/flocculation process for dye removal using sludge from water treatment plant: optimization through response surface methodology, J. Hazard. Mater. 175 (2010) 651–657.
[5] M.X. Zhu, L. Lee, H.H. Wang, Z. Wang, Removal of an anionic dye by adsorption/precipitation processes using alkaline white mud, J. Hazard. Mater. 149 (2007) 735–741.
[6] N. Saffaj, M. Persin, S.A. Younsi, A. Albizane, M. Cretin, A. Larbot, Elaboration and characterization of microfiltration and ultrafiltration membranes deposited on raw support prepared from natural Moroccan clay: application to filtration of solution containing dyes and salts, Appl. Clay Sci. 31 (2006) 110–119.
[7] S. Sachdeva, A. Kumar, Preparation of nanoporous composite carbon membrane for separation of Rhodamine B dye, J. Membr. Sci. 329 (2009) 2–10.
[8] K.M. Majewska-Nowak, Application of ceramic membranes for the separation of dye particles, Desalination 254 (2010) 185–191.
[9] C.S.D. Rodrigues, L.M. Madeira, R.A.R. Boaventura, Optimization of the azo dye Procion Red H-EXL degradation by Fenton's reagent using experimental design, J. Hazard. Mater. 164 (2009) 987–994.
[10] H.S. El-Desoky, M.M. Ghoneim, R. El-Sheikh, N.M. Zidan, Oxidation of Levafix CA reactive azo-dyes in industrial wastewater of textile dyeing by electro-generated Fenton's reagent, J. Hazard. Mater. 175 (2010) 858–865.
[11] S. Raghu, C.A. Basha, Chemical or electrochemical techniques, followed by ion exchange, for recycle of textile dye wastewater, J. Hazard. Mater. 149 (2007) 324–330.
[12] J. Labanda, J. Sabaté, J. Llorens, Modeling of the dynamic adsorption of an anionic dye through ion-exchange membrane adsorber, J. Membr. Sci. 340 (2009) 234–240.
[13] R. Sanghi, A. Dixit, P. Verma, S. Puri, Design of reaction conditions for the enhancement of microbial degradation of dyes in sequential cycles, J. Environ. Sci. 21 (2009) 1646–1651.
[14] Z.J. Li, X.W. Zhang, J. Lin, S. Han, L.C. Lei, Azo dye treatment with simultaneous electricity production in an anaerobic–aerobic sequential reactor and microbial fuel cell coupled system, Bioresour. Technol. 101 (2010) 4440–4445.
[15] W.Y. Yang, A.M. Li, C. Fu, J. Fan, Q.X. Zhang, Adsorption mechanism of aromatic sulfonates onto resins with different matrices, Ind. Eng. Chem. Res. 46 (2007) 6971–6977.
[16] D. Xu, S. Hein, S.L. Loo, K. Wang, The fixed-bed study of dye removal on chitosan beads at high pH, Ind. Eng. Chem. Res. 47 (2008) 8796–8800.
[17] D. Kaušpėdienė, E. Kazlauskienė, A. Gefenienė, R. Binkienė, Comparison of the efficiency of activated carbon and neutral polymeric adsorbent in removal of chromium complex dye from aqueous solutions, J. Hazard. Mater. 179 (2010) 933–939.
[18] K.C. Maheria, U.V. Chudasama, Sorptive removal of dyes using titanium phosphate, Ind. Eng. Chem. Res. 46 (2007) 6852–6857.
[19] D. Karadag, M. Turan, E. Akgul, S. Tok, A. Faki, Adsorption equilibrium. Kinetics of reactive black 5 and reactive red 239 in aqueous solution onto surfactant-modified zeolite, J. Chem. Eng. Data 52 (2007) 1615–1620.
[20] S. Pirillo, M.L. Ferreira, E.H. Rueda, Adsorption of alizarin, eriochrome blue black R, and fluorescein using different iron oxides as adsorbents, Ind. Eng. Chem. Res. 46 (2007) 8255–8263.
[21] Y. El Mouzdahir, A. Elmchaouri, R. Mahboub, A. Gil, S.A. Korili, Adsorption of methylene blue from aqueous solutions on a Moroccan clay, J. Chem. Eng. Data 52 (2007) 1621–1625.
[22] P.K. Mohapatra, D.S. Lakshmi, A. Bhattacharyya, V.K. Manchanda, Evaluation of polymer inclusion membranes containing crown ethers for selective cesium separation from nuclear waste solution, J. Hazard. Mater. 169 (2009) 472–479.
[23] O. Duman, E. Ayranci, Attachment of benzo-crown ethers onto activated carbon cloth to enhance the removal of chromium, cobalt and nickel ions from aqueous solutions by adsorption, J. Hazard. Mater. 176 (2010) 231–238.
[24] L. Janus, G. Crini, V. El-Rezzi, M. Morcellet, A. Cambiaghi, G. Torri, A. Naggi, C. Vecchi, New sorbents containing beta-cyclodextrin. Synthesis, characterization, and sorption properties, React. Funct. Polym. 42 (1999) 173–180.
[25] G. Crini, Studies on adsorption of dyes on beta-cyclodextrin polymer, Bioresour. Technol. 90 (2003) 193–198.
[26] A. Romo, F.J. Peñas, J.R. Isasi, Sorption of dibenzofuran derivatives from aqueous solutions by β-cyclodextrin polymers: an isosteric heat approach, J. Colloid Interface Sci. 279 (2004) 55–60.
[27] G. Crini, H.N. Peindy, Adsorption of C.I. Basic Blue 9 on cyclodextrin-based material containing carboxylic groups, Dyes Pigments 70 (2006) 204–211.
[28] I.X. García-Zubiri, G. González-Gaitano, J.R. Isasi, Isosteric heats of sorption of 1-naphthol and phenol from aqueous solutions by β-cyclodextrin polymers, J. Colloid Interface Sci. 307 (2007) 64–70.
[29] E.Y. Ozmen, M. Yilmaz, Use of β-cyclodextrin and starch based polymers for sorption of Congo red from aqueous solutions, J. Hazard. Mater. 148 (2007) 303–310.
[30] A. Romo, F.J. Peñas, J.R. Isasi, I.X. García-Zubiri, G. González-Gaitano, Extraction of phenols from aqueous solutions by β-cyclodextrin polymers. Comparison of sorptive capacities with other sorbents, React. Funct. Polym. 68 (2008) 406–413.
[31] E.Y. Ozmen, M. Sezgin, A. Yilmaz, M. Yilmaz, Synthesis of β-cyclodextrin and starch based polymers for sorption of azo dyes from aqueous solutions, Bioresour. Technol. 99 (2008) 526–531.
[32] M. Chen, L. Cui, C.H. Li, G.W. Diao, Adsorption, desorption and condensation of nitrobenzene solution from active carbon: a comparison of two cyclodextrin and two surfactant, J. Hazard. Mater. 162 (2009) 23–28.
[33] E. Yilmaz, S. Memon, M. Yilmaz, Removal of direct azo dyes and aromatic amines from aqueous solutions using two β-cyclodextrin-based polymers, J. Hazard. Mater. 174 (2010) 592–597.
[34] HB. Li, Y.Y. Chen, The sol–gel technique to prepare calix[6]crown-containing organosilicon resins and their adsorption properties towards metal ions, React. Funct. Polym. 55 (2003) 171–178.
[35] A. Yilmaz, E. Yilmaz, M. Yilmaz, R.A. Bartsch, Removal of azo dyes from aqueous solutions using calix[4]arene and β-cyclodextrin, Dyes Pigments 74 (2007) 54–59.
[36] F.F. Yang, H.Y. Guo, X.Q. Cai, X.L. Chen, Syntheses and adsorption properties of novel calixarene polymers: Calix[6]-1-4-crown-4-based netty polymers, React. Funct. Polym. 64 (2005) 163–168.
[37] T. Oshima, R. Saisho, K. Ohe, Y. Baba, K. Ohto, Adsorption of amino acid derivatives on calixarene carboxylic acid impregnated resins, React. Funct. Polym. 69 (2009) 105–110.
[38] M.A. Kamboh, I.B. Solangi, S.T.H. Sherazi, S. Memon, Synthesis and application of calix[4]arene based resin for the removal of azo dyes, J. Hazard. Mater. 172 (2009) 234–239.
[39] K.A. Connors, The stability of cyclodextrin complexes in solution, Chem. Rev. 97 (1997) 1325–1357.
[40] A.F. Danil de Namor, R.M. Cleverley, M.L. Zapata-Ormachea, Thermodynamics of calixarene, Chem. Rev. 98 (1998) 2495–2525.
[41] Y. Liu, C.C. You, H.Y. Zhang, Supermolecular Chemistry, NanKai University Press, China, 2001.
[42] S.D. Richardson, C.S. Wilson, K.A. Rusch, Use of rhodamine water tracer in the marshland upwelling system, Ground Water 42 (2004) 678–688.
[43] R. Jain, M. Mathur, S. Sikarwar, A. Mittal, Removal of the hazardous dye Rhodamine B through photocatalytic and adsorption treatments, J. Environ. Manage. 85 (2007) 956–964.
[44] S. Shinkai, S. Mori, H. Koreishi, T. Tsubaki, O. Manabe, Hexasulfonated calix[6]arene derivatives: a new class of catalysts, surfactants, and host molecules, J. Am. Chem. Soc. 108 (1986) 2409–2416.
[45] S. Shinkai, K. Araki, T. Tsubaki, T. Arimura, O. Manabe, New syntheses of calixarene-p-sulphonates and p-nitrocalixarenes, J. Chem. Soc., Perkin Trans. 1 11 (1987) 2297–2299.
[46] B. Karagozoglu, M. Tasdemir, E. Demirbas, M. Kobya, The adsorption of basic dye (Astrazon Blue FGRL) from aqueous solutions onto sepiolite, fly ash and apricot shell activated carbon: kinetic and equilibrium studies, J. Hazard. Mater. 147 (2007) 297–306.
[47] M. Turabik, Adsorption of basic dyes from single and binary component systems onto bentonite: simultaneous analysis of basic red 46 and basic yellow 28 by first order derivative spectrophotometric analysis method, J. Hazard. Mater. 158 (2008) 52–64.
[48] P. Janos, Sorption of basic dyes onto iron humate, Environ. Sci. Technol. 37 (2003) 5792–5798.
[49] K.P. Singh, D. Mohan, S. Sinha, G.S. Tondon, D. Gosh, Color removal from wastewater using low-cost activated carbon derived from agricultural waste material, Ind. Eng. Chem. Res. 42 (2003) 1965–1976.
[50] S. Lagergren, Zur theorie der sogenannten adsorption gelöster stoffe, K. Sven. Vetenskapsakad Handl., vol. 24, 1898, pp. 1–39.
[51] Y.S. Ho, G. McKay, Pseudo second order model for sorption process, Process Biochem. 34 (1999) 451–465.
[52] Y.S. Ho, Review of second-order models for adsorption systems, J. Hazard. Mater. 136 (2006) 681–689.
[53] I. Langmuir, The constitution and fundamental properties of solids and liquids, J. Am. Chem. Soc. 38 (1916) 2221–2295.
[54] I. Langmuir, The adsorption of gases on plane surfaces of glass, mica and platinum, J. Am. Chem. Soc. 40 (1918) 1361–1403.
[55] H.M.F. Freundlich, Über die adsorption in lösungen, Zeitschrift für Physikalische Chemie 57 (1906) 385–471.
[56] J.L. Lu, M.Y. Wu, X.L. Yang, Z.B. Dong, J.H. Ye, D. Borthakur, Q.L. Sun, Y.R. Liang, Decaffeination of tea extracts by using poly(acrylamide-co-ethylene glycol dimethylacrylate) as adsorbent, J. Food Eng. 97 (2010) 555–562.